Journal of Radioanalytical and Nuclear Chemistry (2018) 315:195–206
https://doi.org/10.1007/s10967-017-5647-6

Effective adsorption of U(VI) from aqueous solution using magnetic chitosan nanoparticles grafted with maleic anhydride: equilibrium, kinetic and thermodynamic studies

Hamza Shehzad[1] · Limin Zhou[1] · Zhao Li[1] · Quanshui Chen[1] · Yun Wang[1] · Zhirong Liu[1] · Adesoji A. Adesina[2]

Received: 26 September 2017 / Published online: 5 December 2017

Abstract

The in situ formed magnetite nanoparticles was encapsulated by maleated chitosan to synthesize a novel magnetic chitosan nano-sorbent (MCN-MA) for the effective sorption of uranium. The sorption kinetics could be described by the pseudo-second-order model, whereas the sorption isotherms could be fitted to the Langmuir model (q_m = 187.9 mg/g). The MCN-MA showed higher U(VI) sorption capacities (compared to MCN) due to high affinity of carboxylate groups introduced from grafting maleic anhydride. Thermodynamic parameters indicate that U(VI) sorption is endothermic and feasible. The nano-size and magnetic property of the MCN-MA allow its efficient U(VI) sorption and facile magnetic separation from wastewaters.

Keywords Chitosan · Maleic anhydride · Magnetic nano-sorbent · U(VI) · Sorption

Introduction

The mining of uranium ores and their hydrometallurgical processing produce aqueous waste streams which contains different kinds of radionuclides. Also during the chemical leaching of uranium from waste ores using sulfuric acid, a part of uranium is inevitably released into the natural environment [1]. The pollution of U(VI) concentrated in spent fuel or dispersed in mine tailings has become a worldwide concerned problem. Meanwhile, the uranium resources are rather limited and the expected shortage of uranium in the near future contribute to make the recovery/separation of uranium a strategic issue [2]. A number of processes have been developed for U(VI) removal/recovery, including reductive precipitation [3], solid-phase extraction [4], membrane separation [5], solvent extraction [6], ion exchange [6, 7], and sorption [1, 2, 8–11]. Among these methods, adsorption, a simple and mild reaction process, has been considered as the most effective and potential treatment method for environmental pollutants, it is easy to operate and can be applied in large scale for possible practical applications [9, 10].

The sorption using natural polymer (such as chitosan) has attract great attention for researchers in recent years [2, 8, 12, 13]. Chitosan is an abundant biopolymer which has some unique properties such as biodegradability, biocompatibility, and non-toxicity. This material is widely used in water treatment and purification. The amino and hydroxyl functional groups in chitosan are responsible for metal sorption since they are able to form complexes with many heavy metal ions [12–17]. Therefore, chitosan reveals a very promising starting material for manufacturing chelating resins [13].

Magnetic chitosan sorbents (MCS) are a significant improvement over conventional sorbents that have been used to treat polluted water. Chitosan, the basic matrix material comprising MCS, is biocompatible and economic. Chitosan can also be modified with various chelating

Electronic supplementary material The online version of this article (https://doi.org/10.1007/s10967-017-5647-6) contains supplementary material, which is available to authorized users.

✉ Limin Zhou
minglzh@sohu.com

✉ Quanshui Chen
qshchen@ecit.cn

[1] State Key Laboratory for Nuclear Resources and Environment, East China University of Technology, 418 Guanglan Road, 330013 Nanchang, People's Republic of China

[2] School of Chemical Sciences and Engineering, University of New South Wales, Sydney 2035, Australia

ligands for selective and efficient binding to particular pollutants. Traditional adsorbents, such as activated carbon, ion exchange resins, and biosorbents, require complex separation techniques. The advantages of MCS include: (i) low-cost natural polymer as the matrix material; (ii) fast adsorption rate; (iii) high efficiency; (iv) high capacity for specific target pollutants; (v) environmentally friendly; and (vi) easy magnetic separation.

The poor porosity of traditional chitosan-based sorbents is the limiting property of these sorbents for the sorption of metals. To improve mass transfer properties, an efficient way is to decrease the size of the particles or change the conditioning of the biopolymer (such as gel or foams). Nano-sorbents possess excellent sorption performance due to their high specific surface area and the absence of resistance to intraparticle diffusion [13]. However, the nano-sorbents are difficult to be separated from treated effluents for recovering the spent materials; this problem can be solved by associating magnetic cores (immobilized in polymeric shell) to the nano-sorbents: the spent materials can thus be recovered after sorption by magnetic separation (using a magnet) [18].

In order to enhance the sorption capacity or selectivity for target metals, a highly efficient method is to graft new functional groups on the backbone of chitosan [2, 8]. The O/N containing groups (Lewis base) are reported to be very efficient for complexing metal ions (Lewis acid). Different O/N-containing chemicals such as diethylenetriamine [14], tetraethylenepentamine [15], methacrylamide [16], poly (itaconic acid) [17], poly(acrylic acid) [19], and amino acids [8] have been grafted onto chitosan for enhancing sorption. Maleic anhydride (MA) has been used for the modification of different supports (such as styrene–divinylbenzene [20], chitosan/TiO_2 [21], and cellulose [22]) to improve metal sorption properties. The advantages of maleic anhydride as a modifier include: (i) easy introduction of carboxylate groups as the sorption sites; (ii) a relatively cheap cost for the modifier; (iii) facile modification of chitosan under mild reaction conditions. Moreover, in this work, the MA is grafted onto the MCN sorbents using homogeneous grafting method, in this way more functional groups could be uniformly introduced onto the chitosan matrix. The common post-modification for the preparation of the sorbents can only introduce functional groups on the surfaces of the sorbents.

In this work, the magnetic chitosan nano-sorbents functionalized with maleic anhydride (MCN-MA) were synthesized and used for efficient U(VI) sorption. The functionalized magnetic sorbents bear chelating O/N-containing groups (Lewis base) which are responsible for U(VI) (Lewis acid) sorption. The sorption isotherms, uptake kinetics and thermodynamic properties of MCN-MA for U(VI) sorption were investigated. The isothermal and kinetic parameters are important for the scaling up of the process before investigating sorption properties in continuous systems.

Experimental

Chemicals and reagents

Chitosan (deacetylation degree of 90%) was supplied by Aoxing Bio-technology Co., Ltd (Zhejiang, China). Dimethyl sulfoxide (DMSO), epichlorohydrin, acrylamide, $FeSO_4{\cdot}7H_2O$, $FeCl_3$ and ethanol were Aldrich products. $UO_2(NO_3)_2{\cdot}6H_2O$ were supplied by Jinan Uranium Company (Fuzhou, China). The U(VI) solutions were prepared by appropriate dilution of the stock solutions (1000 mg/L) which were prepared by dissolving amounts of $UO_2(NO_3)_2{\cdot}6H_2O$ in distilled water, after adding some drops of HNO_3 for the acceleration of its dissolution.

Preparation of sorbents

Preparation of maleated chitosan by homogeneous grafting of maleic anhydride

The graft of maleic anhydride onto chitosan was conducted by a similar method reported in Ref. [23]. 2.0 g of chitosan was treated with 90 mL of DMSO and constantly stirred at room temperature. Then, amount of maleic anhydride (1.0–4.0 g) in DMSO solution was added to perform the required reaction at 60 °C for 8 h. The reaction product was cooled to room temperature and subsequently precipitated in 250 mL acetone. Finally, the solid product was filtered, washed with acetone and diethyl ether and then lyophilized for 3 days and dried under vacuum to get the maleated chitosan.

Preparation of magnetic maleated chitosan nanoparticle (MCN-MA)

Magnetic chitosan nanoparticles were prepared by chemical co-precipitation of Fe(III) and Fe(II) under base condition in the presence of maleated chitosan followed by hydrothermal treatment. Maleated chitosan (2 g) was dissolved in 100 mL (20%) CH_3COOH before adding of $FeCl_3$ (3.86 g) and $FeSO_4{\cdot}7H_2O$ (3.31 g) salt-solutions (under 2:1 molar ratio). The black magnetite nano-particles were in situ formed at 40 °C by adding 2 M NaOH dropwisely with constant stirring (the pH was maintained at 10–10.4.) The mixture was heated at 90 °C for 1 h under stirring and separated by decantation. Then, 12 mL of 0.01 M epichlorohydrin (containing 0.067 M NaOH at pH 10.0) was mixed with the freshly prepared wet magnetic

chitosan nanoparticles. The mixture was heated to 50 °C for 2 h under stirring. After reaction, the products were magnetically separated, and rinsed with ethanol and deionized water. For comparison, the magnetic chitosan nanoparticle (MCN) was also synthesized in the same procedure using chitosan (instead of maleated chitosan) as the raw material. The molecular structure and brief synthetic route for MCN-MA are shown in Scheme 1.

Characterization of the sorbents

The chemical composition of the sorbents was conducted using CHNS Vario EL III-elementary analyzer (Elementary, Germany). The morphology of the sorbent was analyzed by a Hitachi H-800 transmission electron microscopy. X-ray diffraction (XRD) patterns were obtained on a XRD-2000 X-ray diffractometer with Cu Kα radiation, in the range $2\theta = 5$–80 °C. The magnetic properties were determined on a Lakeshoper, 730T vibrating sample magnetometer at room temperature. The FTIR spectra were measured on a Nicolet, Magna-550 spectrometer, and the scanning range was set between 4000 and 400 cm^{-1}. Thermal gravimetric analysis of the sorbents was conducted on Shimadzu TGA-50H in the nitrogen flow (heating rate 10 K/min). The zeta potential measurements were performed using a Zeta Potential Analyzer 2000.

Sorption/desorption experiments

The pH effect, sorption isotherms and uptake kinetics for U(VI) sorption onto the sorbents were investigated. The pH of the suspension was adjusted with 0.1–0.4 mol/L HCl or NaOH. The sorption isotherms were conducted at pH 4.5 to avoid possible precipitation. The suspensions containing sorbents and U(VI) solution at a fixed pH and temperature were shaken for 1 h to ensure the sorption equilibrium. The solid was separated from aqueous solution by a magnet, and the residual U(VI) concentration in solution was determined by Arsenazo III spectrophotometric method.

In order to investigate the effect of co-existed ions, the sorbents were mixed with multi-ion solution containing U(VI) ion as well as other co-existed ions (La^{3+}, Ce^{3+}, Ba^{2+}, Sm^{3+}, Gd^{3+}, Nd^{3+}, Mn^{2+}, Co^{2+}, Sr^{2+}, and Ni^{2+}) at

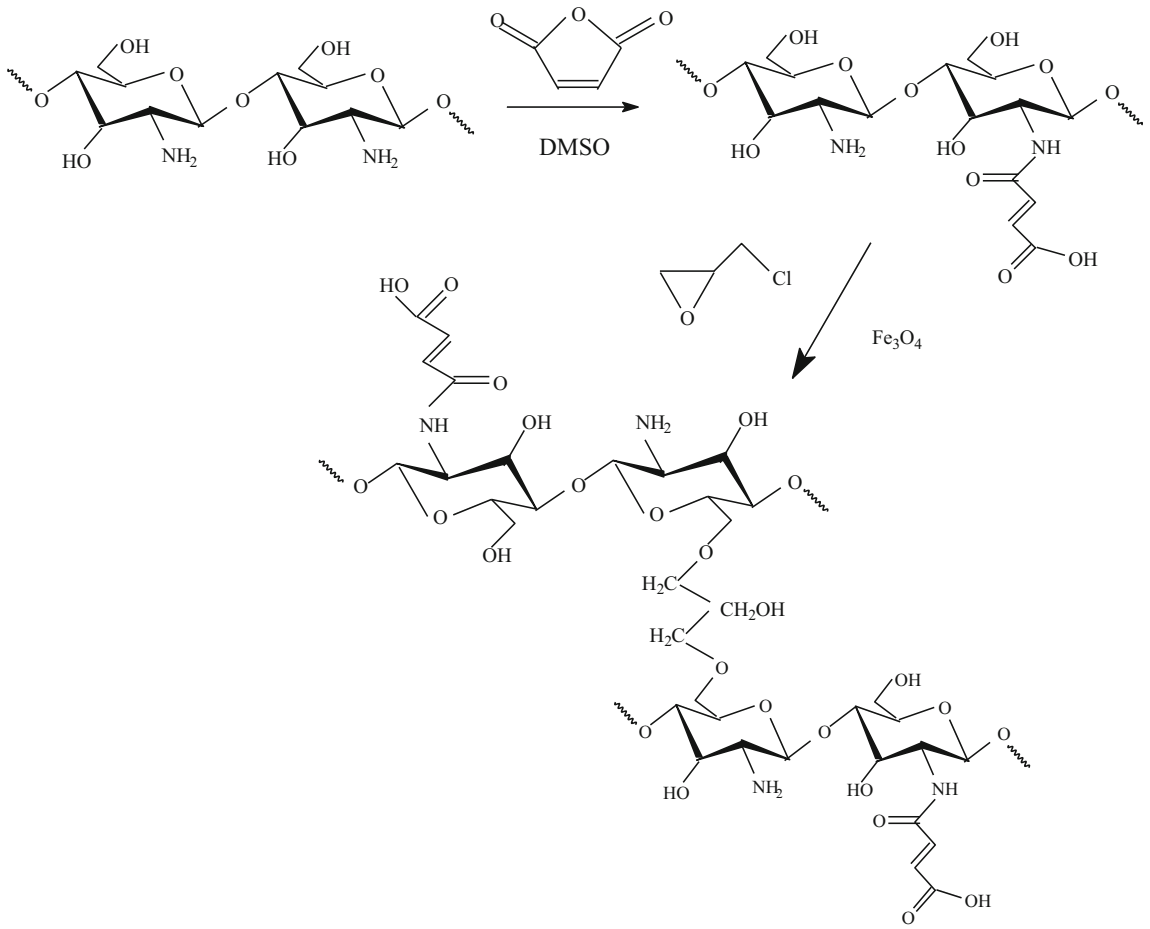

Scheme 1 Synthetic route for MCN-MA

pH 4.5 and 298 K, after being shaken for 1 h, the solutions were separated. The concentrations for the metal ions were determined by inductively coupled plasma atomic emission spectroscopy (ICP–AES, Thermo Elemental, USA).

The desorption of U(VI) from the sorbents was conduct by using acidified thiourea (0.5 M thiourea after adding some drops of HNO_3) as the eluent. The U(VI)-loaded sorbents were mixed with 0.5 M acidified thiourea (pH 2.5) and stirred for 1 h. After magnetic separation, U(VI) concentration in the eluate was determined. The U(VI) sorption/desorption was conducted for consecutive five cycles with the same sorbents to evaluate the reusability of the sorbents.

Results and discussion

Preparation and characterization of the sorbents

Magnetic chitosan nano-based particles were synthesized by a simple one-step method: Fe(II) and Fe(III) ions in chitosan solution was simultaneously precipitated with chitosan after adding NaOH solution. In this procedure magnetic chitosan nano-particles were produced [8, 13]. Chitosan is soluble in acidic solutions due to the protonation of the amine groups; thus it needs to be cross-linked to prevent its dissolving [24]. Glutaraldehyde was not chosen as a crosslinking agent since the amine groups (involving in crosslinking reaction) of chitosan have been already occupied by maleate during the modification of chitosan. Accordingly, epichlorohydrin was selected to crosslink chitosan since it reacts with hydroxyl groups of chitosan. Meanwhile, the maleic anhydride modification of chitosan may increase active sites (such as carboxylate groups) and thus improve the U(VI) sorption capacity. The synthesis route for the magnetic chitosan nano-sorbents are shown in Scheme 1.

The comparison of elemental compositions for both MCN and MCN-MA particles clearly show the effective modification of the sorbents. Indeed, C, H, N contents varied from 29.81, 4.93 and 6.31% for MCN to 28.12, 3.08 and 5.28% for MCN-MA, respectively. The decrease in contents of C, H, and N is due to the grafting of MA onto MCN, which introduces a great number of O-containing groups (–COOH). The –COOH in the MCN-MA is determined to be 2.96 mmol/g for MCN-MA (using the method described in Ref. [25]).

The TEM images (Fig. 1a, b) show the spherical morphology of the sorbents (MCN and MCN-MA): the dark areas correspond to Fe_3O_4, while the bright ones are associated with chitosan (and MA modified chitosan). The magnetic particles are essentially homogeneous in both size and shape. The sorbents were finely dispersed, but some particles tend to form 10–30 nm agglomerate due to the strong magnetic dipole–dipole attraction.

The FTIR spectra of MCN and MCN-MA are shown in Fig. 1c. The characteristic peaks of MCN are identified at 3402 cm^{-1} (overlapped O–H stretch and N–H stretch), 2901 and 2847 cm^{-1} (C–H stretch), 1648 cm^{-1} (NH–CO (I) stretch), 1434 cm^{-1} (N–H bend), 1139 cm^{-1} (bridge –O– stretch), and 1058 cm^{-1} (C–O stretch). The band at 599 cm^{-1} is related to the Fe–O stretching in Fe_3O_4 [13]. The FTIR spectra of MCN-MA presents additional bands: the strong bands at 1720 and 1190 cm^{-1} are assigned to C=O and C–O stretching vibrations of –COOH from maleic acid. Meanwhile, the absorption peak intensity of primary amine (NH_2) groups decreases and shifts to the peak at 1407 cm^{-1} for MCN-MA, indicating the amidization reaction on chitosan amine groups.

The graft of maleic anhydride onto chitosan could be further confirmed in ^1H NMR spectra of chitosan and maleated chitosan (Fig. S1). The ^1H NMR spectra of chitosan shows the typical peaks at 3.44–3.86 ppm, which are attributed to glucosamine unit (H3, H4, H5, H6) of chitosan, the peaks at 3.15 ppm is assigned to H2 and at 2.17 ppm is assigned to the methyl protons of its N-acetyl group, respectively. In the spectra of maleated chitosan, the new peaks at 6.27 and 5.84 ppm are assigned to the methylene protons (–CH=CH–) of N-maleated group, indicating the graft reaction of maleic anhydride onto chitosan.

The XRD patterns for the sorbents (Fig. S2) show eight characteristic peaks corresponding to (111), (220), (311), (400), (422), (511), (440), and (622) indices for Fe_3O_4 nano-particles, this confirms the spinel structure Fe_3O_4 nano-particles encapsulated by chitosan matrix in the sorbents [13, 22]. The sizes of the magnetic nanoparticles were 11.8 and 10.7 nm (calculated from Debye–Scherrer equation [8]) for MCN and MCN-MA, respectively. The magnetization curves (Fig. S3) show typical magnetization loops with no exhibition of remanence and coercivity. The saturation magnetization is 26.5 emu/g for MCN and 22.1 emu/g for MCN-MA, respectively, which is enough for the magnetic separation of the sorbents from the solution [22]. However, these values are much lower than the saturation magnetization of bulk magnetite (about 82 emu/g) due to the embedment of the magnetic cores into a non-magnetic matrix. The difference in the saturation magnetization for the sorbents is due to the different thickness of polymer shell. The magnetic properties of the sorbents make them easy to be separated form solution, and this is very helpful for their use in hazardous environment.

Thermal properties of the sorbents were determined by TGA. As shown in Fig. 1d, MCN exhibits two degradation stages. The initial weight loss of about 10% below 150 °C is due to the loss of free water adsorbed to the material. In

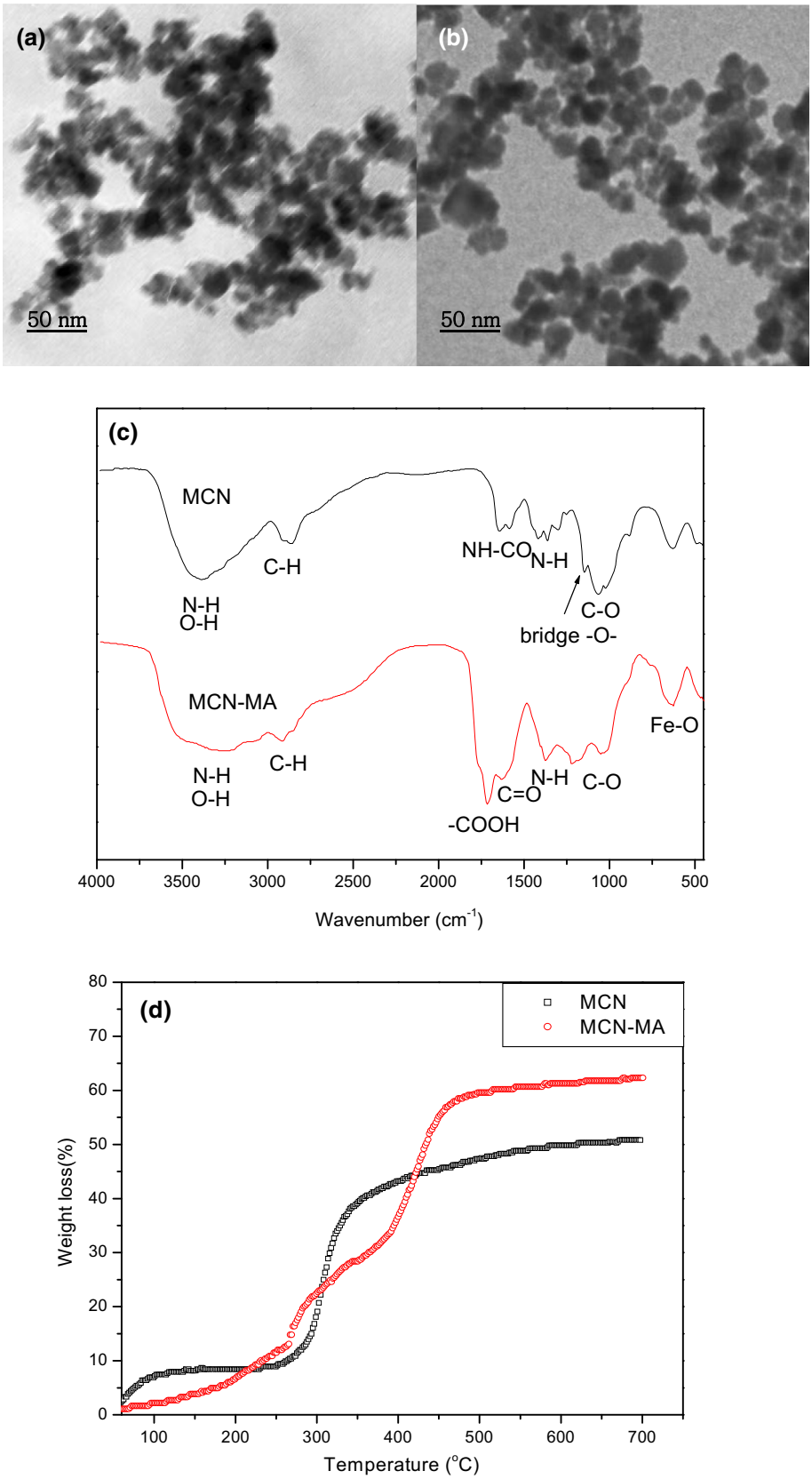

Fig. 1 **a** TEM of MCN, **b** TEM of MCN-MA, **c** FTIR of the sorbents, **d** TG curves of the sorbents

the second stage, the weight loss of 47.9% (started at 245 °C) is attributed to the degradation of glycosidic bond of chitosan [16]. Meanwhile, MCN-MA shows three distinct decomposition stages. The first stage (below 265 °C) with weight loss of 13.1% is due to the evaporation of free water. The second stage (265–370 °C) with weight loss of 17.8% corresponds to the depolymerization of chitosan backbone chain. The third stage (above 370 °C) with weight loss of 32.8% is due to degradation of side chain of MCN-MA. The final weigh loss at 700 °C is 50.9% for MCN and 62.3% for MCN-MA, respectively. The higher weight loss of MCN-MA (compared to MCN) is due to the decomposition of MA which is grafted onto chitosan.

Optimization of maleic anhydride (MA) dosage

The MA dosage has a significant effect on the grafting parameters. To study this, MA dosage was varied from 1.0 to 4.0 g for grafting of chitosan (2.0 g) and the results were presented in Fig. 2. It can be seen that the grafting efficiency sharply increases with increasing MA dosage before reaching a slow increase stage. It can be explained by the fact that as the MA dosage increased, the grafting of the MA on chitosan also increased and this caused higher grafting efficiency and yield. However, beyond a critical value (MA 2.0 g), the grafting efficiency only slightly changed since most of the reactive sites were occupied. Meanwhile, the yield of MA sharply decreases when MA dosage is above 2.0 g. In addition, the preliminary results have shown that the U(VI) sorption capacity is linearly increased with the grafting efficiency (Fig. S4). For simultaneously achieving relatively high grafting efficiency, MA yield, and U(VI) sorption capacity, the MA dosage is optimized as 2.0 g for the preparation of the sorbents.

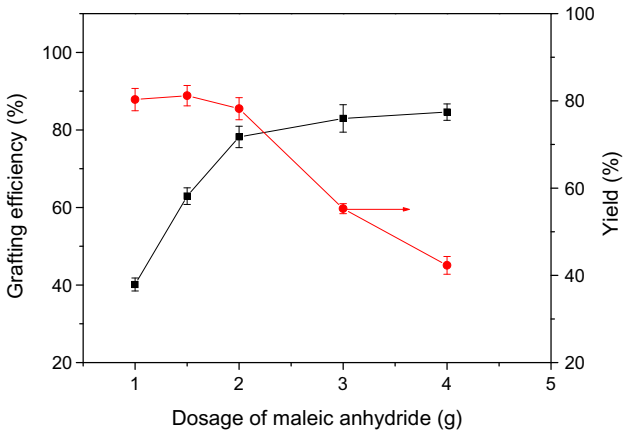

Fig. 2 Effect of MA dosage on the grafting parameters

Adsorption of U(VI)

Effect of pH

The solution pH may influence the dissociation of functional groups (such as carboxyl, amino and hydroxyl groups), the surface charge of the sorbent, and the aqueous chemistry of uranium [13]. The initial solution pH was adjusted by using either 0.1–0.4 M HCl or NaOH solutions. Figure 3 shows the effect of initial pH on U(VI) sorption capacity and equilibrium pH. Apparently, pH has strong impact of on U(VI) sorption: the U(VI) sorption capacity increases from 17.3 to 114.9 mg/g (for MCN) and 41.3 to 178.1 mg/g (for MCN-MA) when the pH increases from 1.5 to 6.5. The variation of the pH during metal sorption (probably due to the acid–base properties of the sorbent) is also shown in this figure: while the pH slightly decreased at pH below 2.0, it sharply increases at pH above 2.5 and stabilizes around pH over 5.0.

In strong acidic solutions, the active sites of the sorbents (amine groups and carboxylate groups) are protonated. In this case, probably U(VI) sorption onto the sorbents is mainly through ion-exchange mechanism:

$$2\text{R-NH}_3^+ + \text{UO}_2^{2+} \rightarrow (\text{R-NH}_2)_2\cdot\text{UO}_2^{2+} + 2\text{H}^+ \quad (1)$$

$$2\text{R-COOH} + \text{UO}_2^{2+} \rightarrow (\text{R-COO}^-)_2\cdot\text{UO}_2^{2+} + 2\text{H}^+ \quad (2)$$

The results of zeta potential measurement for MCN-MA (Fig. S5) indicate that the point of zero charge (pzc) of MCN-MA occurs at pH 4.73. At pH < 4.73 the surface charge of MCN-MA is positive, thus the positive surface of the sorbents enhanced the electrostatic repulsion toward uranyl ions. Besides, the abundant H^+ presented in solution (partly from non-ionized carboxylate groups) also led to a strong competition with uranyl ions for binding sites.

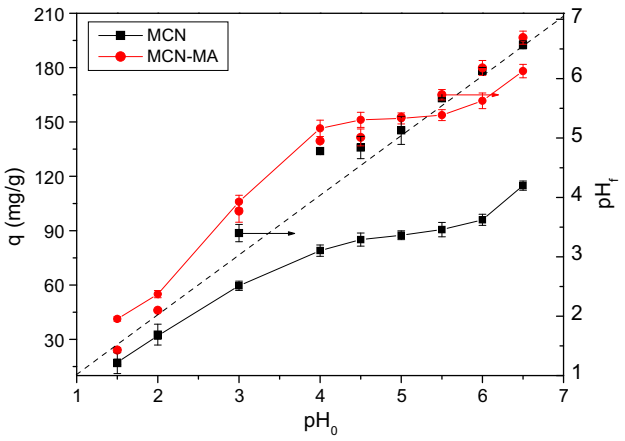

Fig. 3 Effect of initial pH on U(VI) sorption capacity and equilibrium pH (C_0 = 100 mg/L; T = 298 K; t = 1 h; sorbent dosage, SD = 0.25 g/L)

Therefore, U(VI) sorption reduced greatly at low pH. At pH > 4.73 the surface charge of the resin becomes negative, thus the positively charged uranyl ions are adsorbed by electrostatic interaction at pH > 4.73.

In almost neutral condition, the active groups deprotonated and the repulsive forces weakened, thereby enhancing U(VI) adsorption through complexation. The possible complexation mechanism for uranyl ions sorption by MCN-MA is proposed in Scheme 2. The N/O containing groups such as amine and carboxylate groups of the sorbents have a good chelating ability for uranyl ions: the lone pair on N/O atoms (Lewis base) could be supplied to the empty atomic orbital of uranyl ions (Lewis acid), which results in the formation of N/O–UO_2^{2+} complexes. The affinity of MCN-MA for U(VI) sorption is improved through the grafting of MA since it increases the compactness and the volumetric density of O-containing functional groups for chelating sorption. Simsek et al. [26] investigated uranyl sorption on amine-modified maleic anhydride containing terpolymers and proposed the chelation sorption of metal through amine groups as well as carboxylate groups. The rapid increase of sorption capacity at pH > 6.0 probably due to the formation of uranyl hydroxides, including polynuclear and polyhydrolyzed species (such as $UO_2(OH)^+$, $(UO_2)_2(OH)_2^{2+}$, and $(UO_2)_3(OH)_5^+$) and colloidal species $(UO_2)_2(OH)_2$) which can precipitate in the solution or at the surface of the sorbent [2, 8].

At pH > 6.5, precipitation of uranyl ions in the form of $UO_2(OH)_2$ would occur spontaneously, and at pH < 1.5, the inorganic magnetic substance (Fe_3O_4) in the MCN-MA tends to dissolve.

Sorption kinetics

The effect of contact time on U(VI) sorption is shown in Fig. 4. The sorption can be described as a two-stage process: the first stage (contact time < 40 min) which accounts for more than 90% of the total sorption amount, and the second stage that lasts till 180 min of contact. The initial fast sorption stage is attributed to the strong affinity of the reactive groups (amine and carboxylate groups) towards uranyl ions and the small size of magnetic chitosan nano-sorbents which decreases the resistance to intraparticle diffusion and increases the contact of the active sites with adsorbate [8, 13]. The second slow sorption step is due to the strong decrease in the availability of sorption sites since most of them are occupied when the sorption approaches to saturation. The sorption equilibrium was achieved at a contact time of about 40 min: the sorption capacity is stable for longer contact time.

Generally, the sorption process includes successive steps including bulk diffusion, external film diffusion, intraparticle diffusion, and sorption reaction on the active sites [22]. In order to determine the rate-controlling step for U(VI) sorption. The kinetic data were modeled using

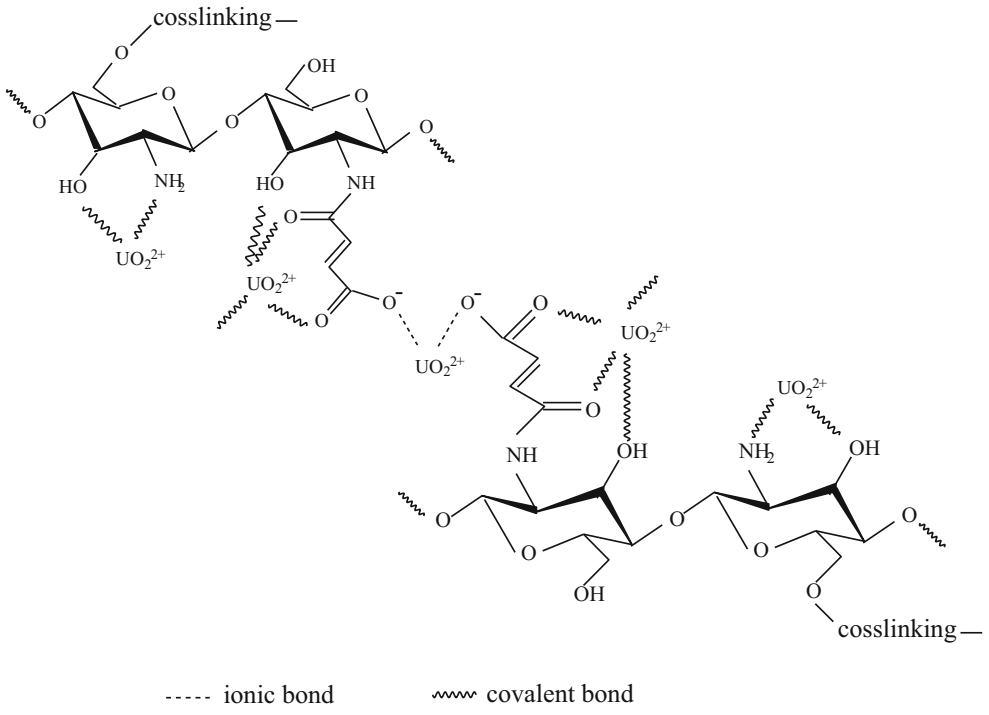

Scheme 2 The possible complexation mechanism for uranyl ions sorption by MCN-MA

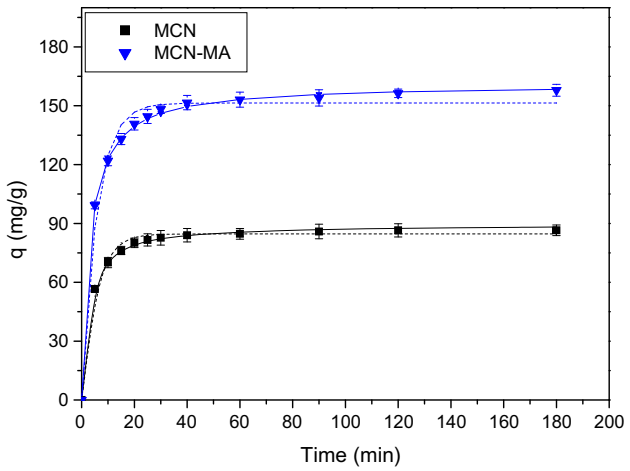

Fig. 4 The sorption kinetic curves for the uptake of U(VI) by MCN-MA and MCN ($C_0 = 100$ mg/L; $T = 298$ K; initial pH = 4.5; SD = 0.25 g/L. The scattered points represent experiment data, the solid lines represent the PSO model and the dash lines represent the PFO model)

kinetic models, such as pseudo-first order model (PFO) (Eq. 3), the pseudo-second order model (PSO) (Eq. 4), and the resistance to intraparticle diffusion (RID) model (Eq. 5) [27, 28]:

$$q_t = q_e(1 - e^{-k_1 t}) \tag{3}$$

$$q_t = \frac{q_e^2 k_2 t}{1 + q_e k_2 t} \tag{4}$$

$$q_t = k_{\text{int}} t^{1/2} + C \tag{5}$$

where q_t and q_e (mg/g) are U(VI) sorption capacities at time t (min) and equilibrium, respectively; k_1 (min^{-1}), k_2 (g mg^{-1} min^{-1}), and k_{int} are the rate constant of PFO, PSO and RID models, respectively.

The parameters of the kinetic models are shown in Table 1. Table 1 clearly shows that the PSO give the best fit of experimental data for both sorbents, indicating chemisorption as the rate-controlling step which involves valence forces for sharing or exchanging electrons through complexation, coordination and chelation between sorbent surface and metal ions [22]. In most cases, the rate constants of PFO and PSO are considered to be ''apparent'' parameters since they integrate the contribution of external and intraparticle diffusion. However, for the magnetic nano-sorbents (MCN and MCN-MA), the thin chitosan shell on the magnetic cores considerably reduces the impact of intraparticle-diffusion resistance. For this reason, RID is not expected to be the rate-controlling step, and this is confirmed by the poor fit of kinetic data for this model.

Sorption isotherms and thermodynamics

Figure 5 shows the U(VI) sorption isotherms for the sorbents (MCN and MCN-MA). The U(VI) sorption capacity increases with increasing U(VI) concentrations, gradually reaching the saturation of the sorbents. The U(VI) sorption isotherms are characterized by the typical "L-shape" curves, indicating that the monolayer sorption for U(VI) ions. The shape of the sorption isotherm with a saturation plateau is consistent with the Langmuir equation, contrary to the Freundlich equation which is characterized by a power-type equation. The U(VI) sorption capacities increase from 151.3 to 174.9 mg/g for MCN-MA with increasing the temperature from 298 to 323 K, indicating that the sorption is endothermic. The sorption equilibrium data were analyzed by various isotherm models including Langmuir, Freundlich, and Dubinin–Radushkevich (D–R) equations [13, 20].

The Langmuir model (Eq. 6) is applied to describe the monolayer sorption which assumes that all the sorption sites are identical and energetically equivalent; whereas the Freundlich isotherm model (Eq. 7) is suitable for heterogeneous sorption, and this model is based on the assumption of an exponential diminution of sorption site energy.

$$q_e = \frac{K_L q_m C_e}{1 + K_L C_e} \tag{6}$$

$$q_e = k_F C_e^{1/n} \tag{7}$$

where C_e (mg/L) is U(VI) equilibrium concentration, q_e and q_m (mg/g) are U(VI) equilibrium sorption amount and saturation sorption capacity, respectively; K_L (L/mg) the Langmuir constant, K_F (mg^{1-n} L^n g^{-1}) and n are the Freundlich constants.

Table 1 Kinetic parameters of the sorption of U(VI) onto MCN and MCN-MA

Sorbents	PFO				PSO			RID		
	$q_{e\ exp}$ (mg/g)	k_1 (min^{-1})	$q_{e\ cal}$ (mg/g)	R^2	$K_2 \times 10^3$ (g/mg/min)	$q_{e\ cal}$ (mg/g)	R^2	K_i (mg/g min$^{-0.5}$)	X	R^2
MCN	84.7	0.196	84.6	0.973	4.25	89.4	0.995	8.10	81.21	0.487
MCN-MA	151.3	0.174	151.4	0.976	2.02	161.1	0.993	4.37	47.03	0.460

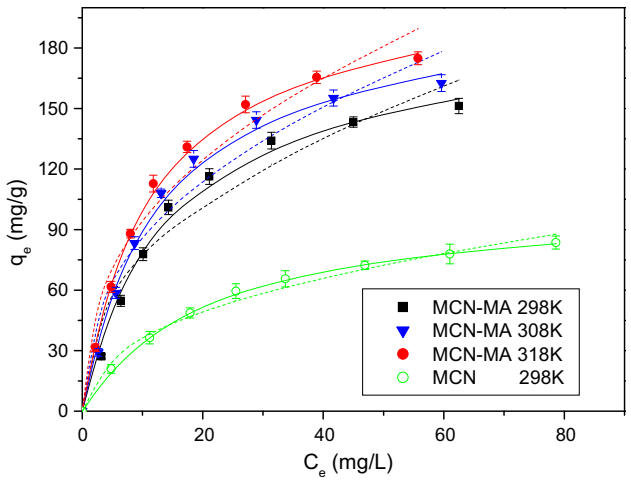

Fig. 5 The Langmuir sorption isotherms for U(VI) sorption onto the sorbents (T = 298–318 K; initial pH = 4.5; SD = 0.25 g/L. The scattered points represent experiment data, the solid lines represent the Langmuir model and the dash lines represent the Freundlich model)

The D–R isotherm model (Eq. 8) is usually used to determine the physical/chemical sorption nature of the sorption process:

$$q_e = q_{DR} e^{K_{DR}\varepsilon^2} \tag{8}$$

where q_{DR} is the saturation sorption capacity for the D–R model, ε is the Polanyi potential [$\varepsilon = RT \ln(1 + 1/C_e)$]. K_{DR} is the constant.

E_{DR} (kJ/mol) is defined as the mean-free sorption energy per molecule of sorbate, this parameter can be determined by:

$$E_{DR} = \frac{1}{\sqrt{-2K_{DR}}} \tag{9}$$

The parameters for different isotherm models are summarized in Table 2. The simulated curves close to experimental points (Fig. 5) confirms the suitability of the Langmuir (correlation coefficient close to 1) for fitting sorption isotherm. For Freundlich model, the exponential term (i.e., $1/n$) is less than 1, indicating that the system is favorable; however, the R^2 values are much lower than those for Langmuir model. The values of mean energy of adsorption (E_{DR} = 11.50–12.02 kJ/mol) are higher than 8 kJ/mol, indicating that sorption proceeds through a chemisorption mechanism [13]. Similarly, Xu et al. [14] proposed the chemisorption mechanism for U(VI) sorption on diethyleneamine-functionalized magnetic chitosan with E_{DR} slightly higher than 9 kJ/mol. In addition, the positive E_{DR} values also indicates the endothermic nature of the sorption process, which is consistent with the positive effect of temperature on U(VI) sorption. The comparative U(VI) adsorption performance by various sorbents are shown in Table 3. It confirms that MCN-MA exhibits relatively high sorption capacity and especially fast uptake kinetics, and this sorbent can be used in new potential adsorption systems.

The thermodynamics parameters, such as Gibbs free energy change ($\Delta G°$), enthalpy change ($\Delta H°$) and entropy change ($\Delta S°$), can be derived from van't Hoff equation [20].

$$\ln K_L = \frac{-\Delta H^o}{RT} + \frac{\Delta S^o}{R} \tag{10}$$

$$\Delta G^o = \Delta H^o - T\Delta S^o \tag{11}$$

where K_L is the Langmuir constant and T is absolute temperature (K).

The values of ΔH^o and ΔS^o were obtained by plotting ln k_L versus $1/T$ (Fig. S6). The thermodynamic parameters are given in Table 4. The positive ΔH^o value (7.37 kJ/mol) confirms the endothermic nature of the sorption process. The endothermic nature of U(VI) sorption has also been reported for other sorbents, such as Amberlite IRA-910 resin [28], tetraethylenepentamine/glycidyl methacrylate chelating resin [35], and salicylideneimine–functionalized hydrothermal carbon [36]. It is possible that some metal ions have to be dehydration before sorption, and this process is endothermic [1, 22]. The negative $\Delta G°$ values indicate that the sorption is spontaneous. Moreover, $\Delta G°$ decreases with increasing the temperature, confirming the positive effect of high temperature on U(VI) sorption. The positive $\Delta S°$ value indicates that the increase in randomness, possibly due to dissociation of complexes, release of

Table 2 Isotherm model parameters for adsorption of U(VI) by MCN-MA and MCN

Sorbents	Temp (K)	Temkin			Freundlich			D–R		
		q_m (mg/g)	k_L (L/mg)	R^2	k_F (mg/g) (L/mg)$^{1/n}$	n	R^2	$K_{DR} \times 10^9$ (J^2/mol^2)	E (kJ/mol)	R^2
MCN-MA	318	213.0	0.088	0.992	37.4	2.48	0.964	3.46	12.02	0.960
	308	201.9	0.081	0.996	33.9	2.47	0.952	3.52	11.91	0.942
	298	187.9	0.073	0.987	30.6	2.46	0.936	3.69	11.64	0.943
MCN	298	104.2	0.049	0.998	14.1	2.39	0.983	3.78	11.50	0.980

Table 3 Sorption capacities and equilibration time for U(VI) sorption by different sorbents

Adsorbents	Equilibration time	Sorption capacity (Mg U/g)	References
Crosslinked chitosan	180	73.7	[29]
Ion-imprinted chitosan/PVA	150	155.8	[30]
Chitosan–tripolyphosphate	4320	235.6	[24]
Cross-linked chitosan with epichlorohydrin	180	49	[31]
Magnetite nanoparticles	300	5	[32]
Magnetic Schiff base	360	94.3	[33]
Magnetic chitosan	40	42	[34]
Magnetic chitosan composite	120	666.7	[10]
Ethylenediamine-modified magnetic chitosan	30	83.8	[11]
Amberlite IRA-910 resin	120	11.9	[28]
Maleic anhydride-functionalized magnetic-chitosan nanoparticles (MCN-MA)	40	187.9	This work
Magnetic-chitosan nanoparticles (MCN)	40	104.2	

Table 4 Thermodynamic parameters of U(VI) by MCN-MA

Temp (K)	$\Delta G°$ (kJ/mol)	$\Delta H°$ (kJ/mol)	$\Delta S°$ (J/mol K)	$T\Delta S°$ (kJ/mol)	R^2
318	− 26.31	7.37	105.91	33.68	0.9836
308	− 25.25			32.62	
298	− 24.19			31.56	

exchangeable ions etc. [22]. In addition, $|\Delta H°| < |T\Delta S°|$ indicates that the adsorption process was dominated by entropy instead of enthalpy changes.

Effect of co-existed ions

To evaluate the sorption selectivity of both MCN and MCN-MA for U(VI) sorption, the sorption experiments were performed in a simulated nuclear industrial effluent with U(VI) and other co-existed ions (Fig. 6). In the presence of competing cations, the total sorption capacity of MCN is 179.1 mg/g for all ions, in which the sorption capacity for U(VI) reaches 41.1 mg/g and is 22.9% of the total sorption amount. As for MCN-MA, the sorption capacity for U(VI) increases to 76.2 mg/g, and the total sorption capacity reaches to 221.3 mg/g, thus resulting in an increase of the selectivity toward U(VI) (34.3% of the total sorption amount). It is reasonable to speculate that the increase in the selectivity for U(VI) is mainly due to the introduction of carboxylic groups onto MCN-MA.

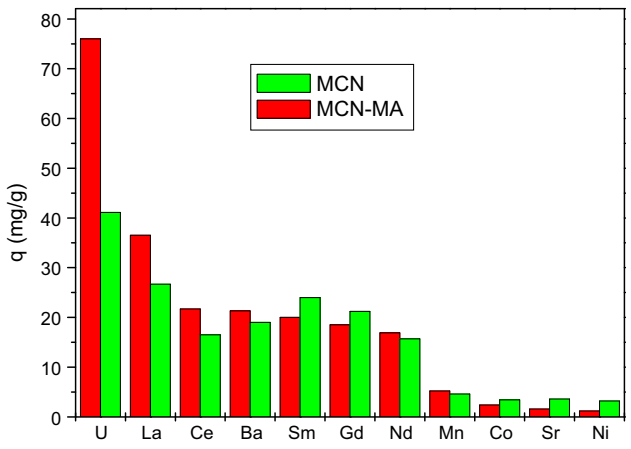

Fig. 6 Competitive adsorption capacities of coexistent ions on MCN and MCN-MA ($C_0 = 100$ mg/L for each metal, $T = 298$ K; initial pH = 4.5; SD = 0.25 g/L). (Color figure online)

Regeneration studies

The desorption of metal ions from U(VI)-loaded sorbents was conducted by using acidified thiourea (0.5 M thiourea acidified with a few drops of HNO_3, at pH 2.5) as the eluent. Thiourea is known as a strong chelating agent for many metal ions. Preliminary tests showed that the acidified thiourea (0.5 M) could efficiently desorbed uranyl ions: 1 h of contact were sufficient for desorption equilibrium. The mechanism of desorption is related to electrostatic and chelation reactions. The desorption efficiency was more than 85% and further increase in thiourea concentration only show negligible improvement for U(VI) desorption. The pure acids such as HCl or HNO_3 are not suggested since these acids may cause the dissolving of the magnetic core of sorbents. The sorption/desorption cycles were repeated for five times. Figure 7 shows the sorption capacity and the sorption efficiency at different cycles: a

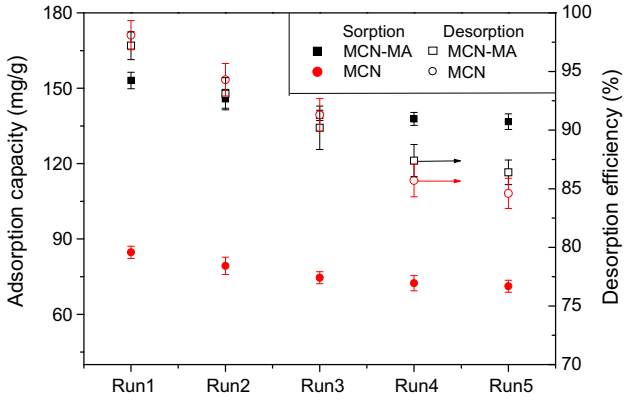

Fig. 7 Different sorption/desorption cycles for the sorbents (C_0 = 100 mg/L for sorption)

progressive decrease in the sorption capacity and the desorption efficiency was observed. However, the sorption capacity decreased by less than 12% at the fifth cycle for MCN-MA. The facile recovery of the sorbent by external magnetic field contributes to make these nano-sorbents very interesting for applications in hazardous environment.

Conclusions

The maleated chitosan magnetic nano-particles (MCN-MA) have been synthesized, characterized and tested for efficient U(VI) sorption from aqueous solution. The interest in using MCN-MA for removal/recovery of U(VI) from aqueous solutions is associated to its unique characteristics, such as relatively high sorption capacities, fast sorption kinetics, and facile magnetic separation. The maximum monolayer sorption capacity obtained from Langmuir model is 187.9 mg/g at 298 K. The sorption kinetics could be modeled with the pseudo-second order model, indicating chemisorption as the main mechanism. The contribution of resistance to intraparticle diffusion is negligible since the nano-size of magnetic sorbents offer large surface areas for U(VI) sorption. The U(VI) sorption on MCN-MA is spontaneous and endothermic. Finally, the sorbents can be efficiently desorbed by acidified thiourea as the eluent and regenerated for several cycles.

Acknowledgements This work was financially supported by the National Natural Science Foundation (21366001; 21667001; 21601033), the International Scientific and Technological Cooperation Projects (2015DFR61020), the Key Research and Development Program and the Natural Science Fund Program of Jiangxi Province (20161BBF60059; S2017ZRMSB0473; GJJ161583).

References

1. Wang X, Fan Q, Yu S, Chen Z, Ai Y, Sun Y, Hobiny A, Alsaedi A, Wang X (2016) High sorption of U(VI) on graphene oxides studied by batch experimental and theoretical calculations. Chem Eng J 287:448–455
2. Elwakeel KZ, Atia AA (2014) Uptake of U(VI) from aqueous media by magnetic Schiff's base chitosan composite. J Clean Prod 70:292–302
3. Gu B, Liang L, Dickey MJ, Yin X, Dai S (1998) Reductive precipitation of uranium(VI) by zero-valent iron. Environ Sci Technol 32:3366–3373
4. Khayambashi A, Wang X, Wei Y (2016) Solid phase extraction of uranium(VI) from phosphoric acid medium using macroporous silica-based D2EHPA-TOPO impregnated polymeric adsorbent. Hydrometallurgy 164:90–96
5. Hoyer M, Zabelt D, Steudtner R, Brendler V, Haseneder R, Repke JU (2014) Influence of speciation during membrane treatment of uranium contaminated water. Sep Purif Technol 132:413–421
6. Sole KC, Cole PM, Feather AM, Kotze MH (2011) Solvent extraction and ion exchange applications in Africa's resurging uranium industry: a review. Solvent Extr Ion Exch 29:868–899
7. Aziz A, Jan S, Waqar F, Mohammad B, Hakim M, Yawar W (2010) Selective ion exchange separation of uranium from concomitant impurities in uranium materials and subsequent determination of the impurities by ICP-OES. J Radioanal Nucl Chem 284:117–121
8. Galhoum AA, Mahfouz MG, Atia AA, Abdelrehem ST, Gomaa NA, Vincent T et al (2015) Amino acid functionalized chitosan magnetic nano-based particles for uranyl sorption. Ind Eng Chem Res 54:12374–12385
9. Yin X, Bai J, Tian W, Li S, Wang J, Wu X (2017) Uranium sorption from saline lake brine by amidoximated silica. J Radioanal Nucl Chem 313:1–9
10. Hritcu D, Humelnicu D, Dodi G, Popa MI (2012) Magnetic chitosan composite particles: evaluation of thorium and uranyl ion adsorption from aqueous solutions. Carbohydr Polym 87:1185–1191
11. Wang JS, Peng RT, Yang JH, Liu YC, Hu XJ (2011) Preparation of ethylenediamine-modified magnetic chitosan complex for adsorption of uranyl ions. Carbohydr Polym 84:1169–1175
12. Pan D, Fan Q, Fan F, Tang Y, Zhang Y, Wu W (2017) Removal of uranium contaminant from aqueous solution by chitosan@attapulgite composite. Sep Purif Technol 177:86–93
13. Galhoum AA, Mahfouz MG, Gomaa NM, Vincent T, Guibal E (2017) Chemical modifications of chitosan nano-based magnetic particles for enhanced uranyl sorption. Hydrometallurgy 168:127–134
14. Xu J, Chen M, Zhang C, Yi Z (2013) Adsorption of uranium(VI) from aqueous solution by diethylenetriamine-functionalized magnetic chitosan. J Radioanal Nucl Chem 298:1375–1383
15. Elwakeel KZ, Atia AA, Guibal E (2014) Fast removal of uranium from aqueous solutions using tetraethylenepentamine modified magnetic chitosan resin. Bioresour Technol 160:107–114
16. Sutirman ZA, Sanagi MM, Karim KJ, Wan AW (2016) Preparation of methacrylamide- functionalized crosslinked chitosan by free radical polymerization for the removal of lead ions. Carbohydr Polym 151:1091–1099
17. Kyzas GZ, Siafaka PI, Lambropoulou DA, Lazaridis NK, Bikiaris DN (2014) Poly(itaconic acid)-grafted chitosan adsorbents with different cross-linking for Pb(II) and Cd(II) uptake. Langmuir 30:120–131

18. Reddy DH, Lee SM (2013) Application of magnetic chitosan composites for the removal of toxic metal and dyes from aqueous solutions. Adv Colloid Interface Sci 202:68–93
19. Li N, Bai R (2006) Highly enhanced adsorption of lead ions on chitosan granules functionalized with poly(acrylic acid). Ind Eng Chem Res 45:7897–7904
20. Ogawa N, Honmyo K, Harada K, Sugii A (2010) Preparation of spherical polymer beads of maleic anhydride–styrene–divinylbenzene and metal sorption of its derivatives. J Appl Polym Sci 29:2851–2856
21. Shaker MA, Yakout AA (2016) Optimization, isotherm, kinetic and thermodynamic studies of Pb(II) ions adsorption onto N-maleated chitosan-immobilized TiO_2 nanoparticles from aqueous media. Spectrochim Acta A 154:145–156
22. Zhou Y, Hu X, Jin Q, Wang X, Ma T (2013) Adsorption of Cd(II) from aqueous solutions by cellulose modified with maleic anhydride and thiourea. Adsorpt Sci Technol 31:583–598
23. Sarkar K, Kundu PP (2012) Preparation of low molecular weight N-maleated chitosan graft-PAMAM copolymer for enhanced DNA complexation. Int J Biol Macromol 51:859–867
24. Sureshkumar MK, Das D, Mallia MB, Gupta PC (2010) Adsorption of uranium from aqueous solution using chitosan tripolyphosphate (CTPP) beads. J Hazard Mater 184:65–72
25. Yusupkhanova M, Shaposhnikova ST, Aikhodzhaev BI (1980) Determination of the carboxyl groups in a copolymer of styrene with maleic anhydride. Fibre Chem 11:417–419
26. Simsek S, Yilmaz E, Boztug A (2013) Amine-modified maleic anhydride containing terpolymers for the adsorption of uranyl ion in aqueous solutions. J Radioanal Nucl Chem 298:923–930
27. Monier M, Ayad DM, Wei Y, Sarhan AA (2010) Adsorption of Cu(II), Co(II), and Ni(II) ions by modified magnetic chitosan chelating resin. J Hazard Mater 177:962–970
28. Rahmati A, Ghaemi A, Samadfam M (2012) Kinetic and thermodynamic studies of uranium(VI) adsorption using Amberlite IRA-910 resin. Ann Nucl Energy 39:42–48
29. Wang GH, Liu JS, Wang XG, Xie ZY, Deng NS (2009) Adsorption of uranium (VI) from aqueous solution onto cross-linked chitosan. J Hazard Mater 168:1053–1058
30. Liu Y, Cao X, Hua R, Wang Y, Liu Y, Pang C, Wang Y (2010) Selective adsorption of uranyl ion on ion-imprinted chitosan/PVA cross-linked hydrogel. Hydrometallurgy 104:150–155
31. Hosoba M, Oshita K, Katarina RK, Takayanagi T, Oshima M, Motomizu S (2009) Synthesis of novel chitosan resin possessing histidine moiety and its application to the determination of trace silver by ICP-AES coupled with triplet automated-pretreatment system. Anal Chim Acta 639:51–56
32. Das D, Sureshkumar MK, Koley S, Mithal N, Pillai C (2010) Sorption of uranium on magnetite nanoparticles. J Radioanal Nucl Chem 285:447–454
33. Zhang X, Jiao C, Wang J, Liu Q, Li R, Yang P, Zhang M (2012) Removal of uranium(VI) from aqueous solutions by magnetic Schiff base: kinetic and thermodynamic investigation. Chem Eng J 198:412–419
34. Stopa L, Yamaura M (2010) Uranium removal by chitosan impregnated with magnetite nanoparticles: adsorption and desorption. Int J Nucl Energy Sci Technol 5:283–289
35. Donia AM, Atia AA, Moussa EM, El-Sherif AM, El-Magied MOA (2009) Removal of uranium(VI) from aqueous solutions using glycidyl methacrylate chelating resins. Hydrometallurgy 95:183–189
36. Wang H, Ma L, Cao K, Geng J, Liu J, Song Q, Yang X, Li S (2012) Selective solid phase extraction of uranium by salicylideneimine-functionalized hydrothermal carbon. J Hazard Mater 229:321–330